Machine Learning Based Predictive Model for AFP Based Unidirectional Composite Laminates

Chathura Wanigasekara, *Student Member, IEEE,* Ebrahim Oromiehie, Akshya Swain, *Senior Member, IEEE,* B. Gangadhara Prusty, and Sing Kiong Nguang, *Senior Member, IEEE*

***Abstract*—Manufacturing of composites using Automated Fibre Placement (AFP) is a complex process which involves large number of processing conditions and variables. Improper selection of these parameters adversely affect the quality and integrity of the manufactured laminates. Thus, it is important to develop a predictive model which can assess how changes in critical process conditions alter the outputs of the manufacturing process. The goal of this investigation is to learn the complex behaviour of composites by developing an intelligent model which can subsequently be used for the prediction of various characteristics of the composites. However, manufacturing of AFP composites is both expensive and time-consuming and therefore the available data samples are less, from the prospective of machine learning, which leads to the *small data learning problem*. This study first solves this problem through Virtual Sample Generation (VSG), then a Neural Network based predictive model is developed to accurately learn the complex relationships between various processing parameters in AFP.**

***Index Terms*—Virtual Sample Generation (VSG), Machine Learning (ML), Automated Fibre Placement.**

I. Introduction

In recent years, the Carbon/Glass Fibre Reinforced Polymer (CFRP/GFRP) based composites are increasingly being used in a wide range of both consumer and industrial applications, including manufacturing of components in automotive and spacecraft due to their lightweight and high strength. Thus, automated manufacturing using robots is critical for mass production [1]. This has created considerable interest within industry groups to adapt AFP based manufacturing to their manufacturing processes considering its high level of productivity, accuracy and reliability. However, AFP is a complicated process where the quality and integrity of the structure depend critically on the proper selection of a large number of variables which are extracted by conducting several coupon level experiments [2], [3], [4].

Proper selection of these processing parameters is essential and has been highlighted by several researchers [5], [6]. Chen and Yousefpour [5] studied the influence of process parameters on the void content and its effects on microstructures. Nixon-Pearson et al. [6] analysed the compaction behaviour of toughened prepregs by studying the void content, both at room temperature debulking and at the elevated temperatures. They reported the void content within the samples consolidated at the room temperature is at the highest level. However, this can be decreased with increase in temperature under compaction which is consistent with hot debulking.

A good understanding of the process parameters and their influences will improve the quality of the manufactured composites. The tuning of these parameters to achieve the desired result is a complex nonlinear optimisation problem and is a significant research concern. In this study, this complex problem has been solved by developing a machine learning (ML) based predictive model for AFP. Note that several parameters (> 50) influence the quality of AFP made composites. These parameters can be categorized into three main groups which include *processing conditions*, *material variables* and *processing defects* as shown in Figure-1. Some of these parameters include, but not limited to, *curing/melting temperature, consolidation force, feed rate, heat flow rate, lay-up speed, material type* and *defect types*. In this investigation, one of the objectives is to obtain a more reliable correlation between the Hot Gas Torch (HGT) temperature and consolidation force by keeping the lay-up speed constant.

In recent years, ML tools have been applied to solve several engineering problems [7], [8], [9], [10], [11]. However, their application to manufacturing is very limited [12], [13], [14]. This is because the success of ML-based algorithms depends on the availability of a large number of data. But due to the high cost of running pilot experiments, the available data samples are often very less [15]. This fails to capture the physics of the manufacturing process. Further, most of the manufacturing processes are continuous and with a small number of experimental data, there exist information gaps. This leads to the *small data learning problem* which needs to be addressed in the first stage of model development. One of the approaches to solving this problem is through Virtual Sample Generation (VSG). Niyogi et al. [16] proved that the process of creating virtual samples (VS) is mathematically equivalent to incorporating prior knowledge. Several researchers have developed various methods for generating VS and used them for the development of models for manufacturing applications. e.g. manufacturing of TFT-LCD [17] and Multi-Layer Ceramic Capacitor (MLCC) [18]. But, the accuracy of these models is dependent on both the techniques of VSG and the ML tools.

The optimum combination of the VSG technique and the ML tool, which gives better accuracy, has recently been investigated by the authors in [19] where they compared the

C. Wanigasekara, A. Swain and S. K. Nguang are with the Department of Electrical, Computer and Software Engineering, The University of Auckland, Auckland, New Zealand., E. Oromiehie and B. G. Prusty are with ARC Training Centre for Automated Manufacture of Advanced Composites, School of Mechanical and Manufacturing Engineering, University of New South Wales, Sydney, Australia. E-mail: c.wanigasekara@auckland.ac.nz, e.oromiehie@unsw.edu.au, a.swain@auckland.ac.nz, g.prusty@unsw.edu.au, sk.nguang@auckland.ac.nz.

Manuscript received April 11, 2019.

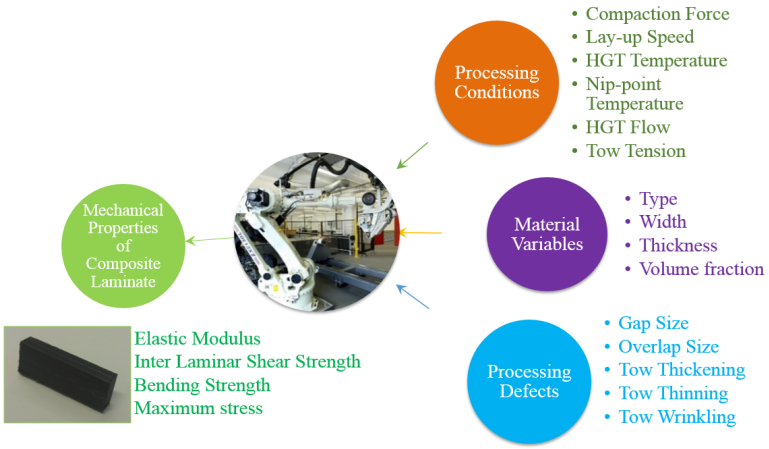

Fig. 1. The parameters that influence the quality of AFP composites.

performance of three VSG methods such as Box-Whisker (BWM-PMCC) method [20], Trend Similarity Assessment (TSA) method [21] and Mega-Trend Diffusion (MTD) method [22] using five well known ML tools such as Back Propagation Neural Network (BPNN), Support Vector Machines (SVM), Multiple Polynomial Regression (MPR), Multiple Linear Regression (MLR) and Regression Tree (RT). It is shown that the combination of the TSA method with BPNN gives the best results [19]. In this study, i) It is established that BPNN based ML gives highest learning accuracy compared to other ML tools when it is trained using VS generated by the TSA method, ii) A predictive model is developed which could successfully predict the complex relationships in AFP based composites.

For the first time, a machine learning based predictive model is developed for AFP manufacturing. However, there is another team of researchers (EC ZAero) working on developing a machine learning tool for metal machining [23]. The focus of this study is on learning the effects of various processing conditions such as disposition rate, HGT Temperature, Nip-Point Temperature and consolidation force on different characteristics of composites, which include elastic modulus, inter laminar shear strength, bending strength and maximum stress using a machine learning based predictive model. The proposed model is generic (scalable) and can easily include the effects of many other processing conditions and parameters on composites characteristics.

The organisation of the paper is as follows: Section-II describes the experimental procedure for collecting AFP data. The method of generating VS is briefly described in Section-III. The efficacy of the proposed predictive model is demonstrated, and the results are presented in Section-IV with conclusions in Section-V.

II. Experiments

The experimental data were collected following several manufacturing stages which include preparation of composite laminates and the extraction of properties of these laminates. Figure-2 shows the schematic of an AFP machine with a Thermoplastic (TP) head in an inset. The machine includes a compaction roller, a heating system and a computer controlled robotic arm [24], [25], [26], [27], [28]. In this process, an incoming tape (A) is bonded to the previously laid and consolidated layer (B) under pressure and temperature which is provided using the compaction roller (C) and the heat source (D), respectively [29]. An HGT based heat source was utilised which delivers high temperature (up to 950 °C) nitrogen (E) through a nozzle around the tape to initiate the polymerisation. The prepreg tapes consist of a bunch of fibres impregnated with resins and are commonly used materials for AFP based manufacturing.

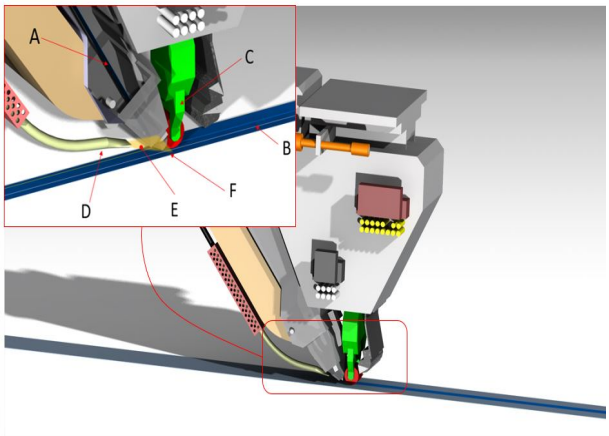

Fig. 2. AFP machine with the TP head. Inset: (A) Incoming tape; (B) Previously laid layer (substrate); (C) Compaction roller; (D) Heat source (HGT); (E) Hot gas; (F) Nip-point.

A. Coupon preparation

For the laboratory based experimental program, 16 samples were manufactured using AFP with individual processing con-

ditions shown in Table-I. In these experiments, the deposition rate was kept constant at 76 mm/s while the temperature and consolidation force were varied. The prepreg tapes were processed by a heating and cooling cycle. Each sample consists of 21 plies of unidirectional thermoplastic prepreg tapes, CF/PEEK (AS4/APC2), supplied by Cytec. The prepreg tapes are $1/4''$ (6.35 mm) wide and 0.15 mm thick, with a fibre volume fraction of 0.6. The overall dimension of each laminate is 200 mm$\times$6.35 mm$\times$3.15 mm. The samples were then cut to test coupon samples (19 mm$\times$6.35 mm$\times$3.15 mm) using a diamond saw. Further details of material properties can be found in [30].

B. Coupon Characterisation

The coupons were loaded into a three-point bend test fixture, specially designed to perform the Short-Beam Strength (SBS)/Interlaminar Shear Strength (ILSS) tests using a uniaxial test machine (Instron-3369-50KN). The test setup used to conduct the SBS/ILSS tests is shown in Figure-3. In these tests, the ratio of the span length to the thickness is kept at 4.0, and the coupon was tested at a constant loading rate of 1 mm/min. Following ASTM D2344 [31], the strength of each coupon was calculated and is expressed as:

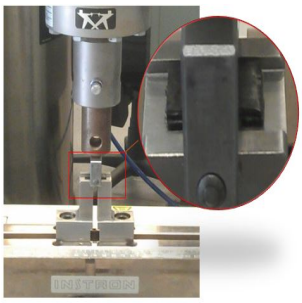

Fig. 3. Experimental set-up for the SBS/ILSS.

$$F^{sbs} = 0.75\frac{P_m}{bh} \tag{1}$$

where F^{sbs} is the short beam strength ; P_m is the maximum flexure load; b is the coupon width and h is the coupon thickness. In addition, the maximum flexural stress and the maximum strain were calculated based on their geometry and are expressed as:

$$\sigma = \frac{3PL}{2bh^2} \tag{2}$$

$$\varepsilon = \frac{6\delta h}{L^2} \tag{3}$$

where σ denotes the stress at the outer surface in the mid-span; L is the support span; P is the applied force; h is the thickness of coupon; b is the width of coupon; ε is the maximum strain at the outer surface and δ is the mid-span deflection.

The summary of the results for mechanical characterisation, which is obtained through the experiments, is illustrated in Figure-4 and the experimental values are shown in Table-II. The failure modes observed during the test were a mixture of inter-laminar shear and plastic deformation including local damages such as delamination and micro-crack between the plies. It is worth to emphasise that the HGT temperature and nip-point temperature are different. The nip-point temperature is the temperature of heated nitrogen at the interface of incoming tape and the substrate, as shown in Figure-2. A nitrogen line supplies nitrogen on the back of the torch, and the nozzle directs the heated nitrogen onto the material. Once the hot gas comes out of the nozzle, temperature drops. The HGT temperature is set on the AFP controller and measured at the tip of the HGT nozzle via a thermocouple.

Further from Table-I and Figure-4, it is observed that for all test conditions, 850 °C HGT processing yield superior elastic modulus, SBS and flexural stress. This observation is consistent with the fact that the actual temperature in this condition is much closer to the process temperature of tape material (382 °C - 400 °C). Consequently, better consolidation takes place under these loading conditions. Higher temperatures, greater than the existing processing temperatures, result in thermal degradation of the polymer (at least above a certain point) which will consequently decrease the SBS/ILSS. Out of all the conditions investigated in this experimental program, it was found that conditions C10 and C12 can provide higher SBS/ILSS compared to others. One of the possible ways to increase SBS/ILSS at lower temperatures is to decrease the deposition rate of the material. This can provide a longer time for the resin to flow and interact with the fibres across the interface.

III. Virtual Sample Generation

Researchers have proposed various methods of virtual sample generation (VSG) from a small number of data samples to solve the small data learning problems which are reported in [15], [17], [18], [20], [21], [22], [32], [33], [34], [35]. Among all these methods, the VSG using triangular membership functions have been very popular due to several advantages [20], [21], [22], [32], [34]. Further, in [19] it has been demonstrated that learning performance of various ML tools is jointly dependent on the VSG method and ML algorithm. The authors in [19] have shown that by combining BPNN with the TSA method, outperforms others. This observation is further established in this study considering three VSG techniques and five popular ML tools. This method is therefore briefly described here for the sake of completeness.

Step 1: For all the attributes (i.e. for all the inputs and outputs), compute the first quartile (Q_1), median (Q_2), third quartile (Q_3) and find the Inter Quartile Range (IQR) from Box-Whisker plots. Let $Q_{1,i}$, $Q_{2,i}$ and $Q_{3,i}$ and denote the first, second and third quartile respectively and IQR_i represents interquartile range of the the i^{th} attribute x_i.

Step 2: Define the triangular membership function of the i^{th} attribute x_i(refer [19]).

$$L_i = \begin{cases} Q_{1,i} - 1.5IQR_i, & \text{if } L_i \leq \min; \\ \min, & \text{if } Q_{1,i} - 1.5IQR_i > \min. \end{cases} \tag{4}$$

TABLE I
THE PROCESSING CONDITIONS OF MANUFACTURED THERMOPLASTIC LAMINATES.

Processing Condition	Deposition Rate (mm/s)	HGT Temp. (°C)	Nip-point Temp. (°C)	Consolidation Force (N)
C1	76	650	215	180
C2				250
C3				350
C4				450
C5		750	315	180
C6				250
C7				350
C8				450
C9	76	850	415	180
C10				250
C11				350
C12				450
C13		950	515	180
C14				250
C15				350
C16				450

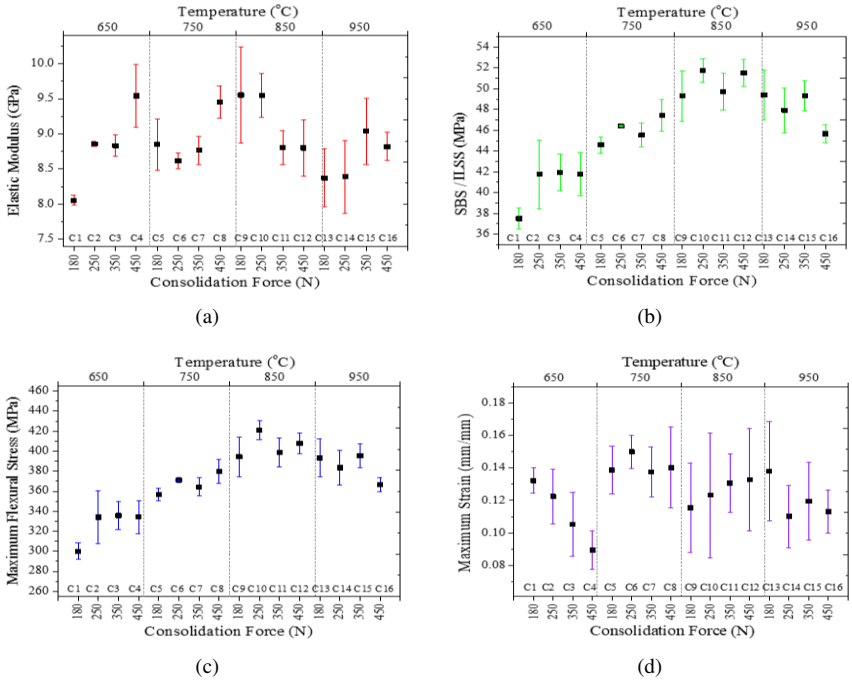

(a) (b) (c) (d)

Fig. 4. The mechanical test results: (a) Elastic Modulus; (b) Short-Beam Strength (SBS); (c) Maximum flexural stress; (d) Maximum flexural strain.

$$U_i = \begin{cases} Q_{3,i} + 1.5IQR_i, & \text{if } U_i \geq \max; \\ \max, & \text{if } Q_{3,i} + 1.5IQR_i < \max. \end{cases} \tag{5}$$

In this equation $'min'$ and $'max'$ corresponds respectively the minimum and the maximum values of the original (experimental) data.

It is worth to note that when the sample size is small, the *parametric average* may not be considered as a good statistical measure. The parameter $Q_{2,i}$ is therefore selected as the centre of the distribution; since it is insensitive to the average [21]. Calculate the value of the membership function of the i^{th} attribute x_i for a particular data point from,

$$\mu(x_i) = \begin{cases} \frac{x_i - L_i}{Q_{2,i} - L_i}, & \text{if } L_i \leq \ x_i < Q_{2,i}; \\ \frac{U_i - x_i}{U_i - Q_{2,i}}, & \text{if } Q_{2,i} \leq x_i \leq U_i; \\ 0, & \text{otherwise.} \end{cases} \tag{6}$$

Step 3: Compute the strength between the different attributes and formulate the TSA matrix as:

$$S = \begin{bmatrix} s_{1,1} & s_{1,2} & \dots & s_{1,n} \\ \vdots & \ddots & & \\ s_{n,1} & s_{n,2} & \dots & s_{n,n} \end{bmatrix} \tag{7}$$

where $s_{i,k}$, $i,k = 1,2,....,n$, is the strength between i^{th} and k^{th} attribute. This is calculated as follows:

$$s_{i,k} = \frac{1}{m}\sum_{j=1}^{m} g_{i,k}(j) \tag{8}$$

where,

$$g_{i,k}(j) = \begin{cases} 1, & \text{if } (x_i(j) - Q_{2,i})(x_k(j) - Q_{2,j}) > 0; \\ 0, & \text{if } (x_i(j) - Q_{2,i})(x_k(j) - Q_{2,j}) = 0; \\ -1, & \text{if}(x_i(j) - Q_{2,i})(x_k(j) - Q_{2,j}) < 0. \end{cases} \tag{9}$$

and number of data samples equals to $'m'$. Note that small values of $s_{i,k}$ implies that there exists weak correlation between the attributes x_i and x_k, where as large values of $s_{i,k}$ shows strong correlation.

Step 4: For all the attributes the VS are generated as follows.

For the 1^{st} attribute v_1, generate N number of VS i.e. $v_1(j), j = 1,2,...,N$ using Plausibility Assessment Mechanism (PAM) which ensures,

$$L_1 \leq \ v_1(j) \leq U_1, j = 1,...,N.$$

The VS for other attributes are calculated progressively from $k = 2,3,.....,n$. VS of the k^{th} attribute is dependent on the VS of the previous attributes, i.e:

$$v_k = f(v_{k-1}, v_{k-2}, ..., v_1) \tag{10}$$

The virtual value (v_k) of the k^{th} attribute x_k is calculated from:

$$v_k(j) = \begin{cases} L_k + \mu(v_i(j))(Q_{2,k} - L_k), & \text{if } s_{i,k} < 0, \text{and } Q_{2,i} < v_i(j) \leq U_i \text{ or if } s_{i,k} > 0, \text{and } L_i \leq v_i(j) < Q_{2,i}; \\ U_k - \mu(v_i(j))(U_k - Q_{2,k}), & \text{if } s_{i,k} < 0, \text{and } L_i \leq v_i(j) \leq Q_{2,i} \text{ or if } s_{i,k} > 0, \text{and } Q_{2,i} \leq v_i(j) \leq U_i; \\ 0, & \text{otherwise.} \end{cases} \tag{11}$$

Note that due to various practical reasons, a slight deviation may occur. In [21], a method has been proposed to account for this probable deviation. For each of the attributes and for every virtual sample, a range of values is defined. The diffusion coefficient $\theta_{i,k}$ between i^{th} and k^{th} attribute is defined as,

$$\theta_{i,k} = -a|s_{i,k}| + b; a, b \in \mathbb{R} \tag{12}$$

When $s_{i,k}$ is small, the possibility v_k to be located on the other end of the median (with respect to v_i) is higher. Further, when $s_{i,k} = 0$,the information between x_i and x_k can not be extracted from observations [21]. The virtual value v_k of k^{th} attribute x_k is therefore generated randomly; since this can lie between L_k and U_k with respect to v_i.

The virtual sample deviation of the i^{th} attribute considering k^{th} attribute can be computed as:

$$v_{i,k}^{-}(j) = \begin{cases} L_i, & \text{if } v_i(j) - \theta_{i,k}(U_i - L_i) < L_i; \\ v_i(j) - \theta_{i,k}(U_i - L_i), & \text{otherwise.} \end{cases} \tag{13}$$

$$v_{i,k}^{+}(j) = \begin{cases} U_i, & \text{if } v_i(j) + \theta_{i,k}(U_i - L_i) > U_i; \\ v_i(j) + \theta_{i,k}(U_i - L_i), & \text{otherwise.} \end{cases} \tag{14}$$

In the next step, the virtual sample deviation range of the k^{th} attribute is computed considering i^{th} attribute $[v_{k,i}^{-}(j), v_{k,i}^{+}(j)]$ as follows:

It is worth to note that the following condition should be satisfied,

$$\mu(v_{k,i}^{+}(j)) = \mu(v_{i,k}^{+}(j)) \tag{15}$$

$$\mu(v_{k,i}^{-}(j)) = \mu(v_{i,k}^{-}(j)) \tag{16}$$

For the k^{th} attribute, its virtual value v_k is calculated from the range $[v_k^{-}(j), v_k^{+}(j)]$ as:

$$[v_k^{-}(j), v_k^{+}(j)] = [v_{k,1}^{-}(j), v_{k,1}^{+}(j)] \cap ... \cap [v_{k,k-1}^{-}(j), v_{k,k-1}^{+}(j)] \tag{17}$$

Note that the generation of $v_i(j)$ is done randomly in the range $[v_i^{-}(j),\ v_i^{+}(j)]$. where,

$$[v_i^{-}(j), v_i^{+}(j)] = [v_{i,1}^{-}(j), v_{i,1}^{+}(j)] \cap ... \cap [v_{i,i-1}^{-}(j), v_{i,i-1}^{+}(j)] \tag{18}$$

IV. Results

The experimental data in Table-II were collected following the procedure mentioned in Section-II and using the processing conditions (parameters) given in Table-I. The goal of this investigation is to find an intelligent model which will accurately encode the learning behaviour of AFP composites and predict the output for different processing conditions. As discussed before, this is essentially a small data learning problem. This is addressed in 2-stages. In this study virtual sample generation is carried out first. For that three VSG methods are considered (TSA, BWM-PMCC, and MTD). Then a comprehensive investigation is carried out to find whether VSG technique or ML tool or combination of the both (VSG and ML) would yield higher accuracy.

The investigation procedure followed in this study is shown in the flowchart of Figure-5 which shows two distinctive cases. This is based on how we select the training and validation data. For **case 1**, the whole VS are used to train the ML tools and the experimental data is used to validate the model. For **case 2**, the whole VS plus a percentage (say 50%) of experimental data is used for training and rest of the experimental samples are used for validation. Further, since the processing conditions in Table-I are sparse, original data used for training has been chosen carefully. Random selection of original data might result in poor performance of the predictive models. Careful selection of a higher percentage of original data will improve the training accuracy. However, validation performance could be poor. To carry out a comprehensive comparison, five popular ML tools (BPNN, MPR, SVM, MLR and RT) are

used. More details about the investigation procedure can be found in [19].

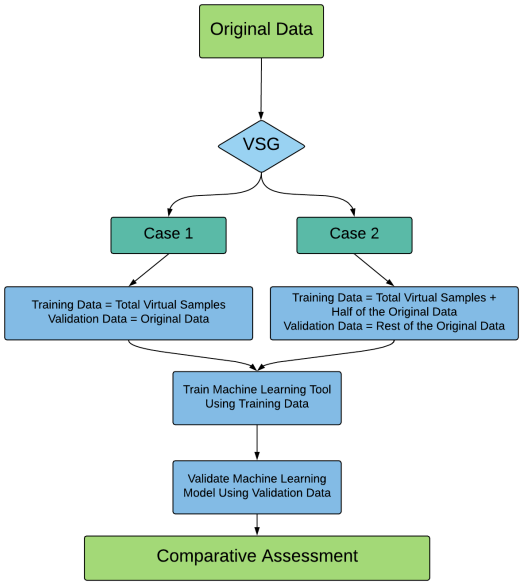

Fig. 5. Investigation procedure.

The comparative performance is assessed using the performance index J,

$$J = \frac{MSE_{Original} - MSE_{VSG}}{MSE_{Original}} \times 100\% \tag{19}$$

where $MSE_{Original}$ and MSE_{VSG} respectively denote the Mean Square Error (MSE) of the models that are fitted only using experimental data and the models that are fitted using VS. Note that the combination of ML tool and the VSG technique that would give higher values of J is better compared to other combinations. The MSE for a particular set of data is calculated as follows:

$$MSE = \frac{1}{M}\sum_{i=1}^{M}(x_i - \hat{x}_i)^2 \tag{20}$$

where M is the number of samples and x_i is the actual value of the sample and $\hat{x}_i$ is the predicted value of the sample.

Considering several synthetic examples, the authors in [19], have shown that the combination of the TSA method of VSG and BPNN gives highest learning accuracy. This is further established with the experimental data. In this study only 4-input variables, dented as, x_1 (HGT Temperature (°C)), x_2 (Consolidation Force (N)), x_3 (Nip-point Temperature (°C)), x_4 (Deposition Rate (mm/s)) and 4-output variables, denoted as, y_1 (Elastic Modulus), y_2 (Short-Beam Strength (SBS)), y_3 (Maximum Flexural Stress), y_4 (Maximum Flexural Strain) are explicitly included. Further, since the Deposition Rate (x_4) is fixed at all times, as it can be seen in Table-I, it is not a persistently exciting input. Also Nip-point Temperature(x_3) follows the same trend as HGT Temperature (x_1) (refer Table-I). Hence HGT Temperature (x_1) can be considered to represent both the inputs HGT Temperature (x_1) and Nip-point Temperature (x_3). Thus, from the perspective of system identification, modelling of AFP can be considered as identification of a 2-input, 4-output process (refer Table-I and Table-II).

Following the procedure outlined in Figure-5, the performance of various VSG methods and ML tools were investigated and the complete predictive model is constructed by cascading the outputs in parallel. The results of this investigation are shown in Tables-III, IV, V, VI, VII, VIII, IX, X for y_1, y_2, y_3 and y_4 (for both cases) respectively.

From the results, it is evident that the learning accuracy for case 2 is higher than case 1. Thus, it is important to use part of the experimental data when the model training is carried out using VS which is demonstrated in Table-IV, Table-VI, Table-VIII and Table-X respectively.

There are significant improvements in the performance of y_2, y_3 and y_4 for case 1. However, all the outputs showed significant improvements in case 2 when compared with $MSE_{Original}$. y_3 recorded the highest improvement showing 81% in case 2 (refer Table-VIII). The performance of the proposed model is validated by comparing the data predicted from the model with the experimental data and are shown for both cases in Table-XI and Table-XII where $y_i, i = 1, 2, 3, 4$ and $\hat{y}_i, i = 1, 2, 3, 4$ denote respectively the measured experimental and predicted outputs.

Note that this predictive model can only estimate outputs with a maximum error of 6.3%, 9.1%, 7.6% and 16% for y_1, y_2, y_3 and y_4 respectively as shown in Table-XII. However, the accuracy can be further increased by including the effects of more number of processing conditions and parameters.

V. Conclusions

In this study, an ML-based predictive model has been developed to predict the manufacturing of composites using the AFP process accurately. Carbon-fibre composite laminates were manufactured using different processing conditions. The mechanical characterisation of AFP fabricated samples was investigated through the laboratory-based mechanical tests. In the predictive model, the processing conditions (lay up speed, HGT temperature, consolidation force) are used as inputs, and the results obtained from the mechanical tests (SBS/ILSS, elastic modulus, etc.) are defined as outputs. To overcome the limitations with small number of experimental data (*small data learning problem*), VS are generated using various methods, and their effectiveness for learning are first studied through comparative investigation using different established ML tools. Among all the VSG methods, the TSA method of VSG, when combined with BPNN, gives the highest learning accuracy. From experimental comparisons, it is evident that the developed predictive model can successfully learn the characteristics of the complex, high-dimensional nonlinear AFP process with a maximum error less than 18% for case-1 and 16% for case-2. Future research will focus on improving the accuracy of the predictive model by incorporating the effects of other processing conditions and parameters. Further, we would explore the possibilities of fitting inverse models using similar procedures used for direct modelling for the AFP manufacturing process.

TABLE II
PARAMETRIC OUTPUTS FOR MANUFACTURING THE THERMOPLASTIC LAMINATES.

Processing Condition	Modulus (MPa)	SBS (MPa)	Max Bending Stress (MPa)	Max Strain
C1	8054.74	37.49	299.93	0.13
C2	8856.14	41.75	334.01	0.12
C3	8831.73	41.94	335.56	0.11
C4	9541.92	41.78	334.27	0.09
C5	8850.71	44.60	356.77	0.14
C6	8615.53	46.38	371.08	0.15
C7	8765.24	45.52	364.16	0.14
C8	9453.16	47.46	379.66	0.14
C9	9551.67	49.30	394.37	0.12
C10	9548.57	51.76	420.69	0.12
C11	8803.02	49.72	398.53	0.13
C12	8799.61	51.51	407.78	0.13
C13	8373.25	49.40	393.18	0.14
C14	8390.93	47.92	383.38	0.11
C15	9038.45	49.32	395.35	0.12
C16	8818.78	45.67	366.50	0.11

TABLE III
PERFORMANCE INDEX J FOR y_1 UNDER DIFFERENT COMBINATIONS OF VSG METHODS AND ML TOOLS-CASE 1

J- AFP y_1	TSA	BWM-PMCC	MTD
BPNN	-1.5%	-79%	-45%
SVM	-37%	-66%	-93%
MLR	-41%	-56%	-81%
RT	-57%	-77%	-139%
MPR	-132%	-214%	-297%

TABLE IV
PERFORMANCE INDEX J FOR y_1 UNDER DIFFERENT COMBINATIONS OF VSG METHODS AND ML TOOLS-CASE 2

J- AFP y_1	TSA	BWM-PMCC	MTD
BPNN	35%	8.7%	-4.2%
SVM	4.8%	-21%	-37%
MLR	3.9%	-23%	-31%
RT	-4.2%	-51%	-59%
MPR	-52%	-196%	-232%

TABLE V
PERFORMANCE INDEX J FOR y_2 UNDER DIFFERENT COMBINATIONS OF VSG METHODS AND ML TOOLS-CASE 1

J- AFP y_2	TSA	BWM-PMCC	MTD
BPNN	48%	13%	3.3%
SVM	11%	9.2%	6.6%
MLR	11%	5.5%	-2.1%
RT	5.1%	-4.9%	-27%
MPR	-8.7%	-53%	-135%

TABLE VI
PERFORMANCE INDEX J FOR y_2 UNDER DIFFERENT COMBINATIONS OF VSG METHODS AND ML TOOLS-CASE 2

J- AFP y_2	TSA	BWM-PMCC	MTD
BPNN	60%	45%	12%
SVM	13%	11%	8.6%
MLR	12%	2.8%	-8.2%
RT	8.9%	-1.2%	-9.6%
MPR	-7.3%	-41%	-103%

TABLE VII
PERFORMANCE INDEX J FOR y_3 UNDER DIFFERENT COMBINATIONS OF VSG METHODS AND ML TOOLS-CASE 1

J- AFP y_3	TSA	BWM-PMCC	MTD
BPNN	57%	42%	20%
SVM	34%	17%	7.8%
MLR	20%	-2.6%	-11%
RT	16%	-9.0%	-15%
MPR	10%	-22%	-98%

TABLE VIII
PERFORMANCE INDEX J FOR y_3 UNDER DIFFERENT COMBINATIONS OF VSG METHODS AND ML TOOLS-CASE 2

J- AFP y_3	TSA	BWM-PMCC	MTD
BPNN	81%	45%	14%
SVM	52%	28%	14%
MLR	41%	16%	-5.2%
RT	23%	-4.1%	-5.9%
MPR	14%	-26%	-72%

ACKNOWLEDGEMENTS

EO and BGP acknowledge the support from ARC Training Centre for Automated Manufacture of Advanced Composites (IC160100040), supported by the Commonwealth of Australia under the Australian Research Councils Industrial Transformation Research Program and CW acknowledge the support from The University of Auckland to carry out this research.

REFERENCES

[1] M. Quddus, A. Brux, B. Larregain, and Y. Galarneau, "A study to determine the influence of robotic lamination programs on the precision

TABLE IX
PERFORMANCE INDEX J FOR y_4 UNDER DIFFERENT COMBINATIONS OF VSG METHODS AND ML TOOLS-CASE 1

J- AFP y_4	**TSA**	**BWM-PMCC**	**MTD**
BPNN	27%	15%	-4.2%
SVM	18%	0.2%	-27%
MLR	1.6%	-39%	-92%
RT	-3.1%	-43%	-49%
MPR	-16%	-181%	-262%

TABLE X
PERFORMANCE INDEX J FOR y_4 UNDER DIFFERENT COMBINATIONS OF VSG METHODS AND ML TOOLS-CASE 2

J- AFP y_4	**TSA**	**BWM-PMCC**	**MTD**
BPNN	56%	28%	17%
SVM	24%	3.6%	1.2%
MLR	9.2%	-5.5%	-40%
RT	-0.8%	-9.2%	-14%
MPR	0.2%	-38%	-106%

TABLE XI
ACTUAL AND PREDICTED VALUES USING VALIDATION DATA CASE 1 (TSA-BPNN)

y_1	$\hat{y_1}$	***% Diff.***	y_2	$\hat{y_2}$	***% Diff.***	y_3	$\hat{y_3}$	***% Diff.***	y_4	$\hat{y_4}$	***% Diff.***
8856.14	9552.62	7.9%	41.75	45.85	9.8%	334.01	353.27	5.8%	0.12	0.142	18%
9541.92	8932.15	6.4%	41.78	45.51	8.9%	334.27	348.31	4.2%	0.09	0.106	18%
8615.53	8290.05	3.8%	46.38	45.42	2.1%	371.08	350.79	5.5%	0.15	0.165	10%
9453.16	9047.01	4.3%	47.46	46.41	2.2%	379.66	368.06	3.1%	0.14	0.130	7.1%
9548.57	8860.74	7.2%	51.76	48.13	7.0%	420.69	468.81	11%	0.12	0.147	23%
8799.61	9186.21	4.4%	51.51	47.35	8.1%	407.78	457.92	12%	0.13	0.149	15%
8390.93	9031.95	7.6%	47.92	46.72	2.5%	383.38	372.47	2.8%	0.11	0.116	5.5%
8818.78	9475.78	7.5%	45.67	47.57	4.2%	366.50	352.80	3.7%	0.11	0.123	12%

TABLE XII
ACTUAL AND PREDICTED VALUES USING VALIDATION DATA CASE 2 (TSA-BPNN)

y_1	$\hat{y_1}$	***% Diff.***	y_2	$\hat{y_2}$	***% Diff.***	y_3	$\hat{y_3}$	***% Diff.***	y_4	$\hat{y_4}$	***% Diff.***
8856.14	9396.66	6.1%	41.75	45.56	9.1%	334.01	346.43	3.7%	0.12	0.136	13%
9541.92	8937.11	6.3%	41.78	45.07	7.9%	334.27	343.81	2.9%	0.09	0.104	16%
8615.53	8273.51	4.0%	46.38	45.45	2.0%	371.08	360.39	2.9%	0.15	0.139	7.3%
9453.16	9179.29	2.9%	47.46	46.46	2.1%	379.66	392.65	3.4%	0.14	0.136	2.9%
9548.57	9009.56	5.6%	51.76	48.72	5.9%	420.69	441.48	4.9%	0.12	0.125	4.2%
8799.61	9053.93	2.9%	51.51	47.94	6.9%	407.78	438.74	7.6%	0.13	0.134	3.1%
8390.93	8817.00	5.1%	47.92	47.16	1.6%	383.38	397.57	3.7%	0.11	0.103	6.4%
8818.78	9194.69	4.3%	45.67	47.14	3.2%	366.50	355.21	3.1%	0.11	0.126	15%

of automated fibre placement through statistical comparisons," in *The* 2^{nd} *International Symposium on Automated Composites Manufacturing, Montreal, Canada*, 2015.

[2] R. Pitchumani, J. W. Gillespie, and M. A. Lamontia, "Design and Optimization of a Thermoplastic Tow-Placement Process with In-Situ Consolidation," *Journal of Composite Materials*, vol. 31, no. 3, pp. 244-275, 1997.

[3] Z. Qureshi, T. Swait, R. Scaife, and H. M. El-Dessouky, "In situ consolidation of thermoplastic prepreg tape using automated tape placement technology: Potential and possibilities," *Composites Part B*, vol. 66, pp. 255-267, Nov. 2014.

[4] H. Bendemra, M. J. Vincent, and P. Compston, "Optimisation of compaction force for automated fibre placement," in 8^{th} *Australasian Congress on Applied Mechanics: ACAM 2014, Melbourne, Australia*, pp. 957-965, Nov. 2014.

[5] J. H. Chen, and A. Yousefpour, "Void formation in thermoplastic composites made by automated fibre placement," in *The* 2^{nd} *International Symposium on Automated Composites Manufacturing. Montreal, Canada*, Apr. 2015.

[6] O. J. Nixon-Pearson, J. P. H. Belnoue, D. S. Ivanov, and S. R. Hallett, "The compaction behaviour of un-cured prepregs," in *The* 20^{th} *International Conference on Composite Materials Copenhagen, Denmark*, July 2015.

[7] R. Rojas, *Neural networks: A systematic introduction*, New York : Springer-Verlag, 1996.

[8] G. Acciani, G. Brunetti, and G. Fornarelli, "Application of Neural Networks in Optical Inspection and Classification of Solder Joints in Surface Mount Technology," *IEEE Transactions on Industrial Informatics*, vol. 2, no. 3, pp. 200-209, Aug. 2006.

[9] A. Giaquinto, G. Fornarelli, G. Brunetti, and G. Acciani, "A Neurofuzzy Method for the Evaluation of Soldering Global Quality Index," *IEEE Transactions on Industrial Informatics*, vol. 5, no. 1, pp.56-66, Feb. 2009.

[10] H. Gao, B. Cheng, J. Wang, K. Li, J. Zhao, and D. Li, "Object Classification Using CNN-Based Fusion of Vision and LIDAR in Autonomous Vehicle Environment," *IEEE Transactions on Industrial Informatics*, vol. 14, pp. 4224-4231, Sep. 2018.

[11] G. Xie, H. Gao, L. Qian, B. Huang, K. Li, and J. Wang, "Vehicle Trajectory Prediction by Integrating Physics- and Maneuver-Based Approaches Using Interactive Multiple Models ," *IEEE Transactions on Industrial Electronics*, vol. 65, pp. 5999-6008, July 2018.

[12] F. Tao, D. Zhao, Y. Hu, and Z. Zhou, "Resource Service Composition and It's Optimal-Selection Based on Particle Swarm Optimization in Manufacturing Grid System," *IEEE Transactions on Industrial Informatics*, vol. 4, no. 4, pp. 315-327, Nov. 2008.

[13] K. Y. Chan, S. Tharam, C. K. Dillon, and C. K. Kwong, "Modeling of a Liquid Epoxy Molding Process Using a Particle Swarm Optimization-Based Fuzzy Regression Approach," *IEEE Transactions on Industrial Informatics*, vol. 7, no. 1, pp. 148-158, Feb. 2011.

[14] F. Tao, L. Yuanjun, L. Xu, and L. Zhang, "FC-PACO-RM: A Parallel Method for Service Composition Optimal-Selection in Cloud Manufacturing System," *IEEE Transactions on Industrial Informatics*, vol. 9, no. 4, pp. 2023-2033, Nov. 2013.

[15] R. Lanouette, J. Thibault, and J. L. Valade, "Process modelling with neural networks using small experimental datasets," *Computers and Chemical Engineering*, vol. 23, no. 9, pp. 1167-1176, 1999.

[16] P. Niyogi, F. Girosi, and T. Poggio, "Incorporating prior information in machine learning by creating virtual examples," *Proceedings of the IEEE*, vol. 86, no. 11, pp. 2196-2209, Nov. 1998.

[17] D. C. Li, C. C. Chen, W. C. Chen, and C. J. Chang, "Employing dependent virtual samples to obtain more manufacturing information in pilot runs," *International Journal of Production Research*, vol. 50, no. 23, pp. 6886-6903, Dec. 2012.

[18] Y. S. Lin, and T. I. Tsai, "Using virtual data effects to stabilize pilot run neural network modelling," *The Journal of Grey System*, vol. 26, no. 2, pp. 84-94, 2014.

[19] C. Wanigasekara, A. Swain, S. K. Nguang, and B. G. Prusty, "Improved Learning from Small Data Sets Through Effective Combination of Machine Learning Tools with VSG Techniques," in *IJCNN, Rio de Janeiro, Brazil*, July 2018.

[20] D. C. Li, W. T. Huang, C. C. Chen, and C. J. Chang, "Employing virtual samples to build early high-dimensional manufacturing models," *International Journal of Production Research*, vol. 51, no. 11, pp. 3206-3224, June 2013.

[21] D. C. Li, W. K. Lin, L. S. Lin, C. C. Chen, and W. T. Huang, "The attribute-trend-similarity method to improve learning performance for small datasets," *International Journal of Production Research*, vol. 55, no. 7 pp. 1898-1913, Apr. 2017.

[22] D. C. Li, C. C. Chen, C. J. Chang, and W. C. Chen, "Employing box-and-whisker plots for learning more knowledge in TFT-LCD pilot runs," *International Journal of Production Research*, vol. 50, no. 6, pp. 1539-1553, Mar. 2012.

[23] G. Gardiner, Zero-defect manufacturing of composite parts, *CompositesWorld*, Jan. 2018. [Online]. Available: https://www.compositesworld.com/blog/post/zero-defect-manufacturing-of-composite-parts. [Accessed: Jul. 2019].

[24] E. Oromiehie, B. G. Prusty, P. Compston, and G. Rajan, "Characterisation of process-induced defects in automated tape placement (ATP) manufacturing of composites using fibre Bragg grating sensors," *Structural Health Monitoring*, vol. 17, no. 1, 2016.

[25] E. Oromiehie, B. G. Prusty, P. Compston, and G. Rajan, "In-situ process monitoring for automated fibre placement using fibre Bragg grating sensors," *Structural Health Monitoring*, vol. 15, no. 6, pp. 706-714, Nov. 2016.

[26] B. G. Prusty, E. Oromiehie, and G. Rajan, *Introduction to Composite Materials and Smart Structures*, ch. 1, New York: CRC Press, 2016.

[27] E. Oromiehie, B. G. Prusty, P. Compston, and G. Rajan, "In-situ simultaneous measurement of strain and temperature in automated fibre placement (AFP) using optical fibre Bragg grating (FBG) sensors," *Advanced Manufacturing: Polymer & Composites Science*, vol. 3, no. 2, pp. 52-61, Apr. 2017.

[28] E. Oromiehie, N. D. Chakladar, G. Rajan, and B. G. Prusty, "Online Monitoring and Prediction of Thermo-Mechanics of AFP Based Thermoplastic Composites," *Sensors*, vol. 19, Mar. 2019.

[29] E. Oromiehie, B. G. Prusty, P. Compston, and G. Rajan, "Automated Fibre Placement based Composite Structures: Review on The Defects, Impacts and Inspections Techniques," *Composite Structures*, vol. 224, Sep. 2019.

[30] E. Oromiehie, B. G. Prusty, P. Compston, and G. Rajan, "The Influence of Consolidation Force on the Performance of AFP Manufactured Laminates," in *International Conference on Composite Materials, China*, Aug. 2017.

[31] ASTM Standard D2344, *Standard test method for short-beam strength of polymermatrix composite materials and their laminates*, ASTM International, West Conshohocken, 2006.

[32] D. C. Li, W. Cheng, C. Chang, C. Chen, and I. Wen, "Practical information diffusion techniques to accelerate new product pilot runs," *International Journal of Production Research*, vol. 53, no. 17, pp. 5310-5319, Apr. 2015.

[33] D. C. Li, and I. H. Wen, "Neurocomputing A genetic algorithm-based virtual sample generation technique to improve small data set learning," *Neurocomputing*, vol. 143, pp. 222-230, June 2014.

[34] C. Huang, and C. Moraga, "A diffusion-neural-network for learning from small samples," *International Journal of Approximate Reasoning*, vol. 35, no. 2, pp. 137-161, 2004.

[35] R. Liu, A. Kumar, Z. Chen, A. Agrawal, V. Sundararaghavan, and A. Choudhary, "A predictive machine learning approach for microstructure optimization and materials design," *Scientific Reports*, vol. 5, pp. 966-982, June 2015.

AUTHORS' BIOGRAPHIES

Chathura Wanigasekara received B.Sc.(Eng.) degree from the University of Peradeniya, Sri Lanka in 2013 and ME Studies degree in Electrical and Electronic Engineering from The University of Auckland in 2016. He is currently a Doctoral student in The University of Auckland. His research interests include nonlinear system identification and control, machine learning & networked control systems.

Ebrahim Oromiehie received Masters & PhD degree from UNSW, Sydney in 2013 and 2018. Currently, he is a Technical officer in the Australian Research Council (ARC) Training Centre for Automated Manufacture of Advanced Composites (AMAC) and also a Postdoctoral Fellow at UNSW Sydney. His major research interests are AFP, online/in-situ process & structural health monitoring.

Akshya Swain received Bsc(Eng) & ME degree in 1985 and 1988. He received Ph.D. degree in Control Engineering from The University of Sheffield in 1997. He is an Associate Editor of IEEE Sensors Journal and Member of the Editorial Board of International Journal of Automation and Control, International Journal of Sensors and Wireless Communications and Control. His research interests include nonlinear system identification and control, machine learning & big data.

B. Gangadhara Prusty is a Professor of Mechanical and Manufacturing Engineering and Director of ARC Centre for Automated Manufacture of Advanced Composites (AMAC) at UNSW Sydney. His research interests are on the nano, micro and macro-mechanics of fibre-reinforced composites, embodied with analytical, experimental and advanced finite element modelling techniques.

Sing Kiong Nguang received BE and PhD degree from The University of Newcastle, Australia, in 1992 and 1995, respectively. He has published over 300 papers in various journals and conferences. He is the Chief-Editor of the International Journal of Sensors, Wireless Communications and Control. His research interests include robust nonlinear control and filtering.